Dual MET and SMO negative modulators overcome resistance to EGFR inhibitors in human non-small cell lung cancer

Floriana Morgillo[‖†]*, Giorgio Amendola[£†], Carminia Maria Della Corte[‖†], Chiara Giacomelli[§], Lorenzo Botta[±], Salvatore Di Maro[£], Anna Messere[£], Vincenza Ciaramella[‖], Sabrina Taliani[§], Luciana Marinelli[±], Maria Letizia Trincavelli[§], Claudia Martini[§], Ettore Novellino[±,] Fortunato Ciardiello[‖], Sandro Cosconati[£]*

[‖]Oncologia Medica, Dipartimento Medico-Chirurgico di Internistica Clinica e Sperimentale "F. Magrassi e A. Lanzara", Università della Campania "Luigi Vanvitelli", Via Pansini 6, 80131 Naples, Italy. [£]DiSTABiF, Università della Campania "Luigi Vanvitelli", Via Vivaldi 43, 81100 Caserta, Italy. [§]Dipartimento di Farmacia, Università di Pisa, Via Bonanno 6, 56126 Pisa, Italy. [±]Dipartimento di Farmacia, Università di Napoli "Federico II", Via D. Montesano 49, 80131 Naples, Italy.

Abstract. Tyrosine kinase inhibitors (TKIs) of the EGF receptor (EGFR) have provided a significant improvement in the disease outcome of non-small cell lung cancer (NSCLC). Unfortunately, resistance to these agents frequently occurs, and it is often related to the activation of the Hedgehog (Hh) and MET signaling cascades driving the epithelial-to-mesenchymal transition (EMT). Since the concomitant inhibition of both Hh and MET pathways restores the sensitivity to anti-EGFR drugs, here we aimed at discovering the first compounds that block simultaneously MET and SMO. By using an "*in silico* drug repurposing" approach and by validating our predictions both *in vitro* and *in vivo*, we identified a set of compounds with the desired dual inhibitory activity and enhanced antiproliferative activity on EGFR TKI-resistant NSCLC. The identification of the known MET TKIs, glesatinib, and foretinib, as negative modulators of the Hh pathway, widens their application in the context of NSCLC.

Introduction

Non-small cell lung cancer (NSCLC) is the major cause of cancer-related deaths worldwide.[1] The primary reason for this poor outcome is the presence of metastatic dissemination in a high proportion of patients at diagnosis. The critical step in the development of metastasis and acquisition of resistance to existing cytotoxic and targeted agents, including EGFR-TKIs, is the epithelial-to-mesenchymal transition (EMT) process. EMT is characterized by a switch from an epithelial phenotype of polarized cells, with the expression of epithelial markers such as E-cadherin, to a mesenchymal phenotype of cells that lack polarity, that are motile, and have E-cadherin down-regulation. This phenomenon has been extensively studied and measures to reverse EMT are awaited to enhance the therapeutic efficacy of anticancer drugs against NSCLC.

In this scenario, the Hedgehog (Hh) signaling cascade has recently emerged as an important mediator of cancer development and metastatic progression.[2] The Hh pathway regulates these processes through the induction of EMT. This pathway is comprised of the ligands Sonic, Indian and Desert hedgehog (Shh, Ihh, Dhh, respectively), the cell surface protein Patched (PTCH) and the Frizzled G protein-coupled receptor (GPCR) Smoothened (SMO). In the absence of Hh ligands, PTCH inhibits SMO; while, upon ligand binding to PTCH, SMO is activated, triggering the GLI1 transcription factor, which in turn migrates into the nucleus, leading to the expression of Hh-induced genes. Hh has been demonstrated to be active in human embryogenesis and in tissue repair, as well as in cancer stem cell renewal and survival. This pathway is also critical for lung development, while its aberrant reactivation is implicated in cellular response to injury and cancer growth.[3,4] Recently, alterations (mutation, amplification, mRNA overexpression) of the gene encoding for SMO have been investigated in The Cancer Genome Atlas (TCGA) lung

adenocarcinomas by whole exome sequencing and were observed in 12.2% of lung tumors. The incidence of SMO mutations was 2.6% and SMO gene amplifications were found in 5% of cases.[5]

Similarly, the overexpression of the receptor tyrosine kinase MET, also called hepatocyte growth factor receptor (HGFR), or/and its activation has been demonstrated to be a crucial mediator of the EMT process and has been implicated in resistance to chemotherapy and to anti-EGFR TKIs. Several MET TKIs inhibitors have been evaluated in phase II/III clinical studies in NSCLC patients, with controversial results.[6] Most probably, blocking MET alone is not sufficient to revert the resistant phenotype as this latter is implicated in several intracellular interactions and the best way to overcome resistance is a combined approach, where the concomitant inhibition of MET and Hh pathways is performed.

In this respect, we have recently demonstrated the occurrence of SMO gene amplification, MET activation and a functional interaction of these two signaling pathways in a model of EGFR-mutated TKI-resistant NSCLC cells.[7] In the same cell model, inhibition of SMO in combination with MET inhibition significantly reduced cancer cell proliferation, induced apoptosis, blocked the invasive and migratory behavior and induced the complete regression of 100% of tumors xenografted in nude mice.[7] Moreover, blockade of Hh pathway reverted EMT and was also associated with enhanced tumor sensitivity to cytotoxic agents in EGFR-wild-type NSCLC models.[7] Consistently, recent data demonstrated that aberrant activation of the Hh pathway represented also a common feature, along with EMT, in an *in vivo* model of acquired resistance to EGFR-inhibitors obtained with a sequence of first-generation (erlotinib), second-generation (afatinib), and third generation (osimertinib) EGFR TKIs.[8]

The synergistic interaction of Hh and MET pathways strongly supports the rationale for a combined therapy in order to overcome resistance to EGFR TKIs. On the other hand, despite the

established pharmacological significance of combination therapies, several advantages can be envisaged with the employment of rationally discovered compounds that are able to simultaneously hit two different pharmacological targets,[9] such as a better description of the pharmacokinetic profile compared to combination therapy, diminished risks of drug–drug interactions, and a simplified dosing scheduling. On the other hand, multitarget compounds might indeed display a degree of target promiscuity resulting in unexpected adverse effects that could lead to late attrition in the drug discovery pipeline. To this end, repurposing of known drugs, with an already described toxicological profile, might indeed offer an attractive opportunity in the search of multitarget ligands.[10]

In this context, the aim of the present study was to rationally discover a set of antiproliferative compounds able to simultaneously block MET and SMO receptors. To this end, we wanted to merge the advantages of the drug repurposing strategy,[10] which searches for novel indications, mechanism of action, and/or pharmacological targets of already existing drugs, with the predictive power of theoretical docking-based virtual screening (VS). Through this "*in silico* drug repurposing approach", we selected, among 1911 MET-inhibitors, a set of 12 promising compounds for their potential dual inhibitory activity against MET and SMO which were validated in *in vitro* and *in vivo* models of resistance to anti-EGFR TKIs.

This strategy allowed us to identify two compounds that are currently in clinical trials, as new inhibitors of the Hh pathway, in addition to the already known AXL and MET inhibitory properties. The potent antitumor activity *in vitro* and *in vivo* in a NSCLC model of EGFR-acquired resistance potentially expands the indications for these two drugs.

Results

***In silico* identification of known MET inhibitors as new SMO binders.**

To identify MET inhibitors, which might show interesting affinities at the SMO receptor and *vice versa*, we took advantage of a public domain repository of compound structures and activity data, the BindingDB database.[11] Thus, a set of 1911 known selective, as well as unselective MET inhibitors, was virtually docked against the available SMO receptor X-ray structures by following a protocol that we recently devised to optimize the performances of structure-based VS against SMO receptor.[12] By following this protocol, we were able to rank the inspected compounds for their predicted affinity against the SMO receptor.

A critical step of a VS campaign is the post-docking selection of the compounds to experimentally test. To this end, we first decided to *in silico* characterize the theoretical interaction pattern established by known SMO antagonists and the published structures for this receptor. Therefore, as happened for the MET inhibitors, a collection of 412 SMO antagonists was also obtained by interrogating the BindingDB database.[11] Thus, by following the above-mentioned docking protocol for these latter compounds the binding pose within the SMO receptor was calculated. These results were subsequently analyzed through an interaction fingerprints routine (see Materials and Methods) thereby allowing us to detect which SMO residues are predicted to be more frequently contacted by the known antagonists for this receptor. According to this inspection, the SMO D384, Y394, R400, and E518 residues are the most frequently contacted ones. Interestingly, also mutagenesis experiments outlined the importance of the above-mentioned residues for SMO antagonist binding.[13] The same interaction pattern was also observed for the docked MET inhibitors within the SMO receptor, thereby substantiating our initial design hypothesis. Figures 1a and 1b depict the interaction fingerprints obtained for the two docking

experiments (SMO antagonists against SMO receptor and MET inhibitors against the same receptor, Figure 1a and 1b, respectively). In addition, analysis of the X-ray antagonist/SMO structures also outlined that N219, F484, and W281 receptor residues provide additional anchoring points for co-crystalized antagonists.
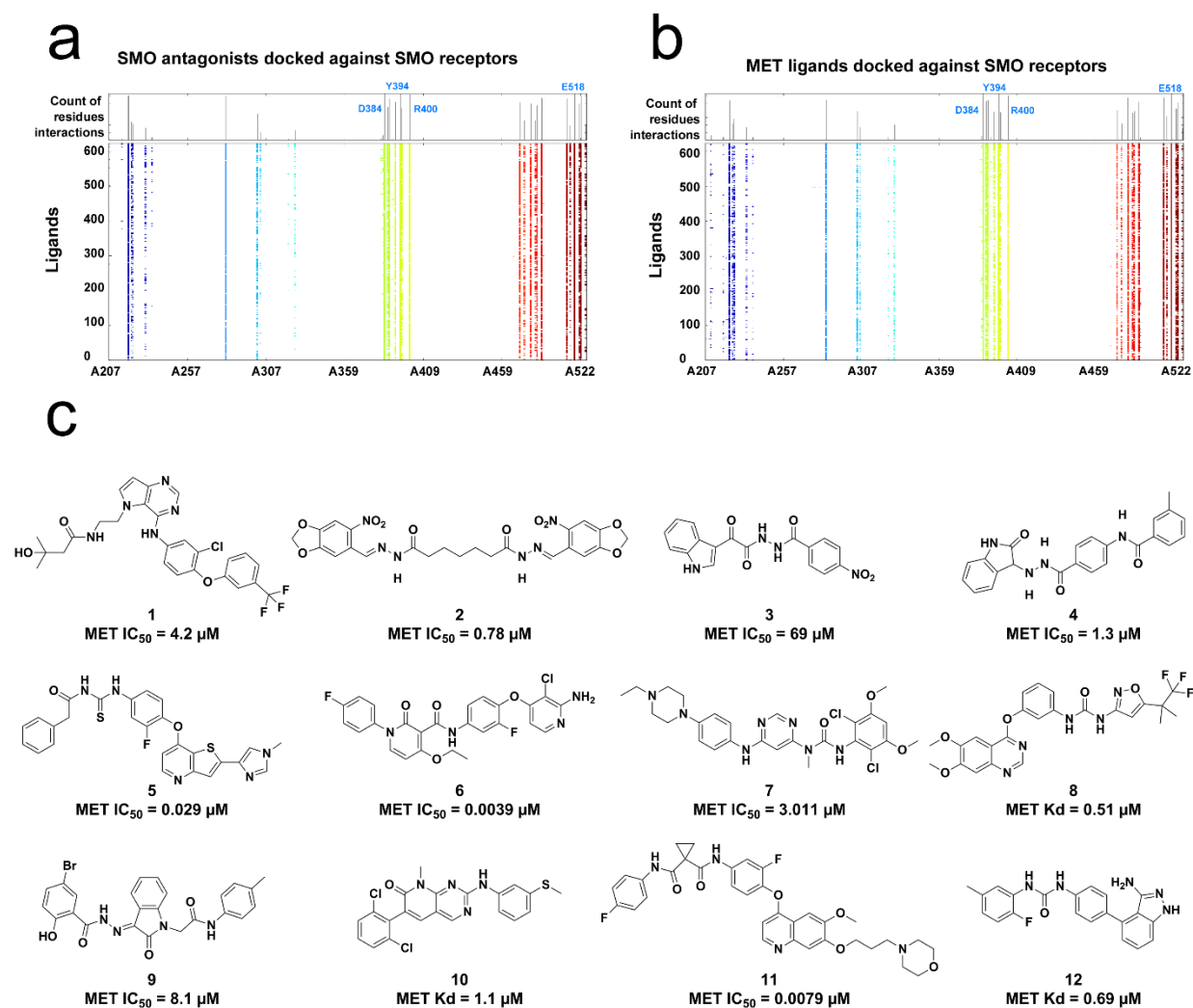

Figure 1. Interaction fingerprints calculated through docking experiments for SMO antagonists (a) and MET inhibitors (b) with the four SMO receptor structures. The most frequently contacted residues are labeled. (c) Structures of the MET inhibitors identified as potential SMO antagonists along with their IC_{50} or K_d values. For each MET inhibitor, the reported IC_{50} or K_d values

correspond to the ones indicated in the paper where they were first published. For compound **1** see ref. 14; for compounds **2**, **4** and **9** ref. 15; for compounds **3**, **5**, **6**, **7**, **8**, **10**, **11,** and **12** see refs. 16, 17, 18, 19, 20, 21, 22, and 23, respectively.

Thus, in our theoretical model, we further filtered out the docked MET inhibitors for which no favorable contacts with the above-mentioned SMO residues were predicted. Of the remaining 421 compounds 25 were commercially available and, of the latter, we decided to select only those whose MET inhibitory potency and or affinity were reported to be at least in the mid-micromolar regimen. This additional filter allowed selecting 12 inhibitors that were finally purchased from different vendors and then checked for compound composition and purity (see Supporting Information). The selected inhibitors along with their reported inhibitory activity and/or affinity against MET are reported in Figure 1c.

Selected MET inhibitors bind and antagonize SMO receptor.

The affinity of the selected compounds towards SMO protein was evaluated by radioligand binding competition studies using [3H]-cyclopamine ((2′R,3S,3′R,3′aS,6′S,6aS,6bS,7′aR,11aS,11bR)-1,2,3,3′a,4,4′,5′,6,6′,6a,6b,7,7′,7'a,8,11,11a,11b-octadecahydro-3′,6′,10,11b-tetramethyl-spiro[9H-benzo[a]fluorene-9,2′(3′H)-furo[3,2-b]pyridin]-3-ol, **13**, Supplementary Chart S1).[24] For this purpose, we used the EGFR exon 19 deletion mutant (delE746-A750) HCC827-GR human NSCLC cell line made resistant to gefitinib *in vitro*, that we previously characterized for SMO and MET expression.[7] The HCC827-GR cell line presents *SMO* gene amplification and MET pathway overexpression and activation.[7] In particular, NGS analysis of this cell line showed a 47% allelic frequency of V404M mutation in the *SMO* gene as compared to the parental HCC827, which showed an allelic frequency of 0.1%, indicating the selection of an

SMO mutated resistant clone during acquisition of resistance to gefitinib. The affinity dissociation constant (K_d) of [^{3}H]-**13** in HCC827-GR cells overexpressing the SMO receptor was 36.9 ± 8.9 nM and a B_{max} of 1567 ± 61 fmol/mg, as obtained by saturation binding studies (Figure 2).
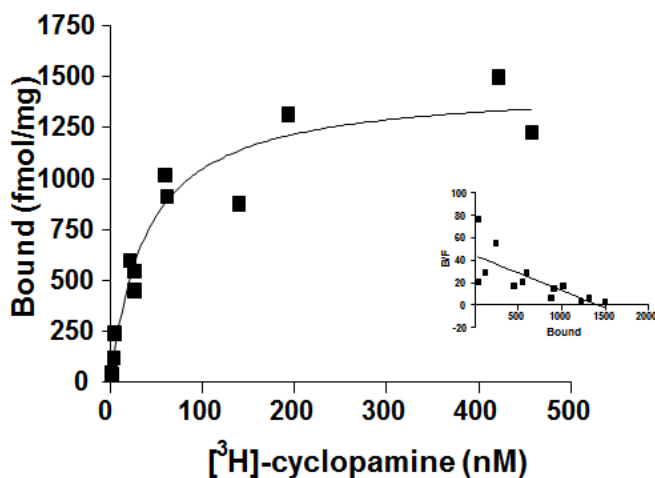

Figure 2. SMO binding analysis. Saturation assay of [^{3}H]-**13** binding to HCC827-GR cells. Cells were incubated 4 h at RT in binding buffer containing increasing concentrations of [^{3}H]-**13**. Non-specific binding was determined in the presence of 25 μM of compound **14**. Scatchard plot analysis of the specific binding. Data are means $\pm$ SEM (n = 3) of a representative experiment over 3 independent experiments. The ability of each of the 12 potential dual inhibitors to displace 25 nM [^{3}H]-**13** specific binding is reported in Table 1.

Table 1. Experimental binding affinity of compounds **1-14** towards V404M mutant SMO receptor in HCC827-GR cells and of compounds **5** and **11** on WT SMO receptor in HEK293T cells.

Compound	K_i V404M SMO (nM)	Ki wt SMO (nM)
1	-	n.d.
2	-	n.d.
3	168.1 ± 21.9	n.d.
4	-	n.d.
5	53.1 ± 9.9	41.7 ± 8.2
6	-	n.d.
7	46.5 ± 6.3	n.d.
8	187.8 ± 36.9	n.d.
9	50.4 ± 11.8	n.d.
10	46.2 ± 11.7	n.d.
11	66.8 ± 7.0	59.7 ± 9.6
12	87.6 ± 12.4	n.d.
13	51.0 ± 8.4	n.d.
14	12.2 ± 1.7	n.d.

n.d. Not determined

The SMO antagonist vismodegib (2-chloro-*N*-[4-chloro-3-(2-pyridinyl)phenyl]-4-(methylsulfonyl)benzamide, **14**,[25] Supplementary Chart S1**)** showed a K_i value of 12.2 ± 1.7 nM in accordance with literature data.[26] Some of the compounds (compounds **1-2**, **4**, and **6**) were not able to completely displace the radiolabeled ligand when tested at a 10 µM concentration. On the contrary, compounds **3**, **5** and **7-12** demonstrated the ability to compete with the [³H]-**13** for the SMO binding site with an affinity in the nanomolar range (Table 1). In particular, compounds **5**

and **11** were demonstrated to be comparably efficient in inhibiting MET and binding SMO. For these latter inhibitors, we also demonstrated that a similar affinity was recorded for the wild-type SMO receptor (Figure 2b), indicating that the V404M SMO mutation does not affect drug affinity. Figure 3 reports the binding mode of compounds **3**, **5**, and **7-12** in the SMO receptor (see Figures S1-8 in Supporting Information for the 2D diagrams of the calculated complexes).
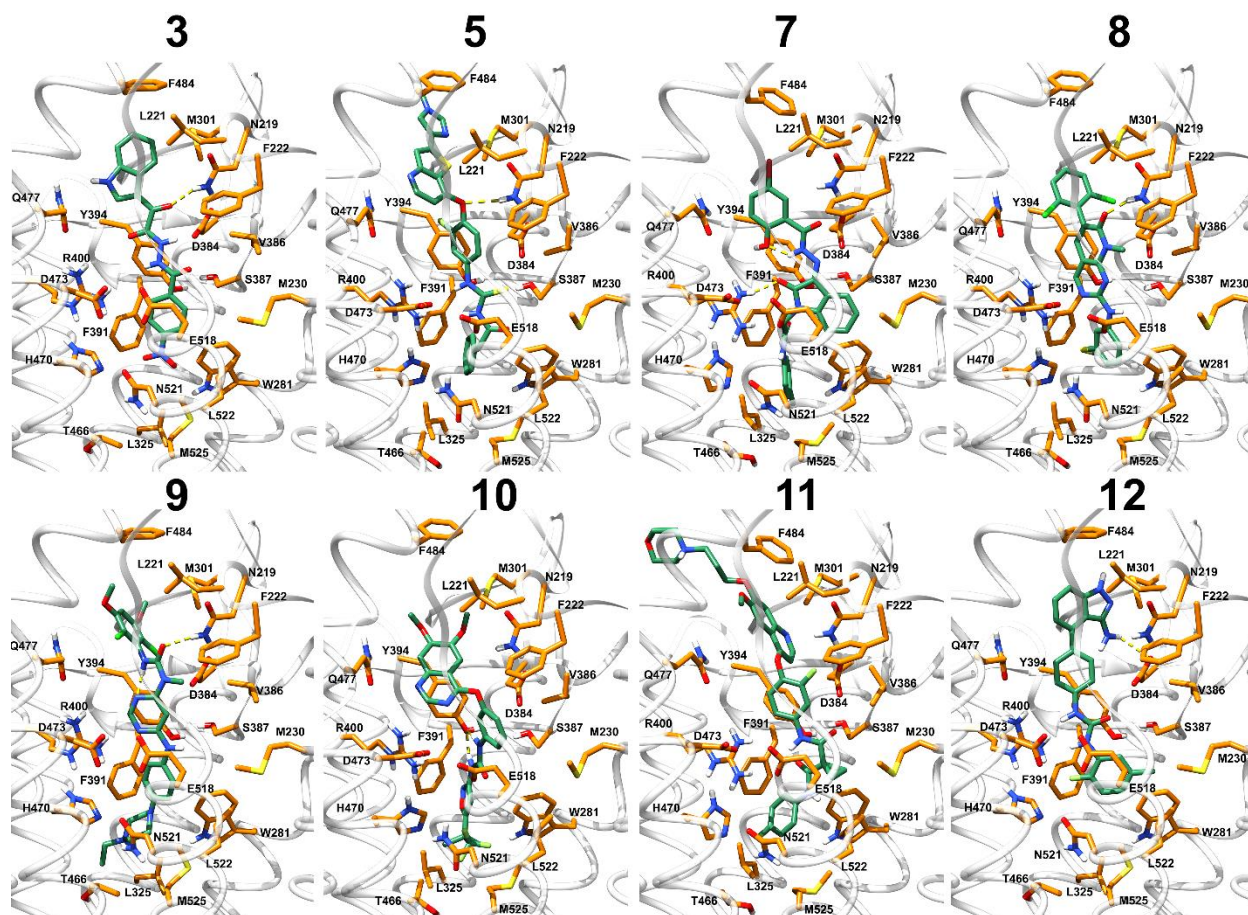

Figure 3. Predicted binding pose of compound **3**, **5**, **7-12** in the SMO X-ray structure. Compounds are represented as green sticks while receptor as orange sticks and transparent white ribbons. H-bonds are represented as dashed yellow lines.

Since GLI1 is a SMO regulated transcription factor,[27] we tested the functional significance of treatment with MET inhibitors that demonstrated the highest ability to displace **13** from binding

to the SMO receptor on GLI1 activity by using a GLI1-responsive promoter within a luciferase reporter expression vector. In particular, we performed a dose-dependent analysis of luciferase activity in HCC827-GR cell line (Figure 3). Treatment with 2 µM (Figure 4a) or 60 µM (Figure 4b) of each compound resulted, respectively, in a 25- to 50% and in a 10- to 100% decrease in GLI1-responsive promoter compared with the HCC827-GR untreated cells ($p < 0.001$).
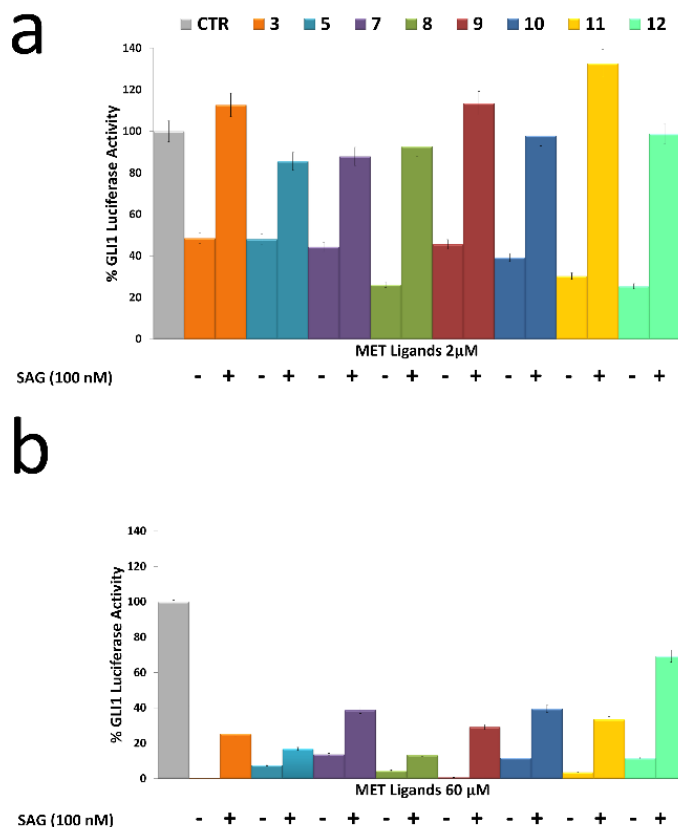

Figure 4. GLI1-driven luciferase expression in HCC827-GR cells during treatment with compounds **3**, **5**, and **7-12** at 2 (**a**) and 60 µM (**b**) and in combination with SAG at a concentration of 100 nM. CTR bars represent the response obtained for HCC827-GR untreated cells.

These data demonstrate that the tested MET inhibitors have a SMO antagonist activity in a concentration-dependent manner. Furthermore, to test if the effect of the selected compounds on

GLI1 activity was mediated by SMO antagonism, we analyzed the ability of the SMO agonist SAG, (100 nM) [*N*-methyl-*N*'-(3-pyridinylbenzyl)-*N*'-(3-chlorobenzo[b]thiophene-2-carbonyl)-1,4 diaminocyclohexane][28] to revert this effect. Interestingly, in the presence of SAG, the induced inhibition of GLI1 activity was completely reverted in almost all treatments at a 2 µM concentration of compounds **3**, **5**, and **7-12** (p<0.01) (Figure 4a) and partially reverted at a 60 µM concentration (Figure 4b), confirming that the selected MET inhibitors antagonize the SMO receptor function.

Dual MET/SMO inhibitors are potent antiproliferative agents in EGFR-TKI resistant human NSCLC.

We then selected, among the 12 potential dual inhibitors, compounds **5** and **11** as the most active MET inhibitors with the most potent activity also on SMO. Moreover, we also kept compounds **6** (significant inhibitory activity against MET and no binding at SMO receptor) and **9** (weak MET inhibitor and nanomolar affinity for SMO) as negative controls. Of interest, compound **5** was identified as glesatinib (*N*-[(3-fluoro-4-{[2-(5-{[(2-methoxyethyl)amino]methyl}pyridin-2-yl)thieno[3,2-b]pyridin-7-yl]oxy}phenyl)carbamothioyl]-2-(4-fluorophenyl)acetamide),[17] MGCD265, Mirati Therapeutics), a tyrosine kinase inhibitor of MET and AXL, and compound **11** as foretinib (*N*1'-[3-fluoro-4-[[6-methoxy-7-(3-morpholinopropoxy)-4-quinolyl]oxy]phenyl]-*N*1-(4-fluorophenyl)cyclopropane-1,1-dicarboxamide, XL880, Exelixis, GSK1363089, GlaxoSmithKline),[22] known as a MET and VEGFR2 inhibitor, with activity against AXL.

We analyzed the activity of **5** and **11** in the *EGFR*-mutated HCC827-GR NSCLC cells with the already described amplification of SMO and overexpression of MET and displaying a typical mesenchymal behavior.[7] In this model, as already demonstrated, activation of AXL (phospho-

AXL), which is a known pathway responsible for the acquisition of resistance to anti-EGFR TKIs and mediator of EMT,[29] and another signaling pathway potentially activated as a resistance mechanism, was not significantly high as compared to sensitive cell models.[7]

We first evaluated the antiproliferative effects at different concentrations of **5** and **11** by using an MTT assay. To compare the effects of each compound with those obtained with specific SMO and MET inhibitors, we also treated the same cancer cells with sonidegib (*N*-[6-[(2*S*,6*R*)-2,6-dimethylmorpholin-4-yl]pyridin-3-yl]-2-methyl-3-[4-(trifluoromethoxy)phenyl]benzamide, NVP-LDE225, SMO antagonist with no reported inhibitory activity against MET, Novartis, **15,** Supplementary Chart S1)[30] and PHA-665752 ((3*Z*)-5-[(2,6-dichlorophenyl)methylsulfonyl]-3-{[3,5-dimethyl-4-[(2*R*)-2-(pyrrolidin-1-ylmethyl)pyrrolidine-1-carbonyl]-1*H*-pyrrol-2-yl]methylidene}-1*H*-indol-2-one, MET inhibitor with no reported activity against SMO, Pfizer, **16,** Supplementary Chart S1)[31] as single agents and in combination. In addition, down-regulation of MET and SMO mRNA levels was performed with silencing-RNA technology. By using drug concentrations ranging from 0.01 to 5 μM, treatment with **5** or **11** resulted in a dose-dependent inhibition of cancer cell growth and showed the lowest IC_{50} values (0.08 and 0.5 μM, respectively for **5** and **11**) (Figure 5a).
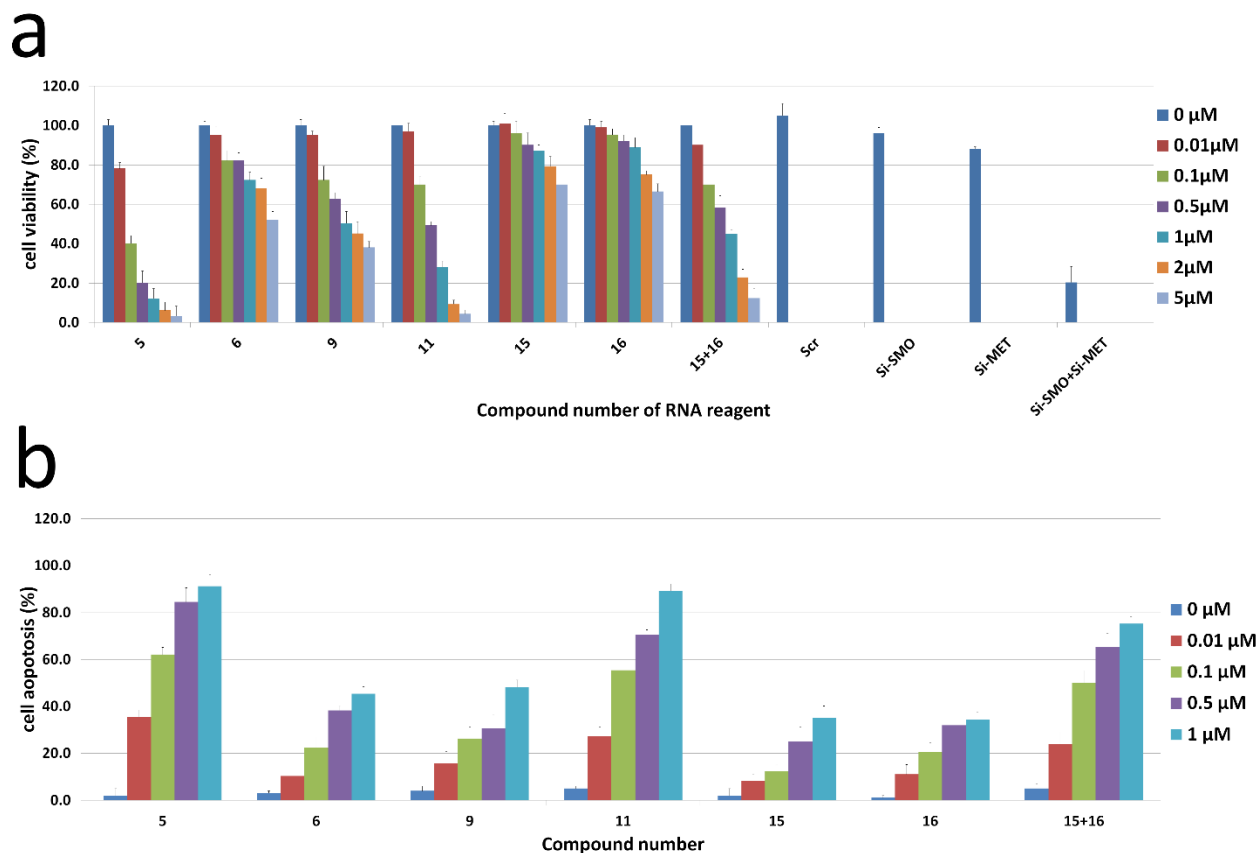
Figure 5. Biological activity of experimental compounds on the HCC827-GR NSCLC cell line. (**a**) MTT Proliferation assay performed on NSCLC HCC827-GR cells with the indicated treatments. The results are the average ± s.d. of three independent experiments, each done in triplicate. (**b**) Apoptosis was evaluated as described in the experimental section with Annexin V staining in HCC827-GR cancer cells, which were treated with the indicated concentration of drugs. Columns, mean of 3 identical wells of a single representative experiment; bars, top 95% confidence interval.

Compounds **6** and **9** resulted in higher IC_{50} values, while the selective inhibition of MET or SMO, by pharmacological or mRNA silencing approaches, did not exert comparable effects. Of interest, **5** and **11** performed even better than combined treatment with **15** and **16** or the double silencing of SMO and MET in resistant cells.

We further asked whether the increased antiproliferative effect induced by **5** and **11** would be the result of an increased apoptosis. Therefore, we analyzed the induction of apoptosis in the EGFR-mutated HCC827-GR cell line after 72-hour treatment. As shown in Figure 5b, flow cytometric analysis revealed that treatment with compound **5** and **11** significantly increased by several-fold the percentage of apoptotic cells in all tested cell lines. For instance, in HCC827-GR cells **5** induced the higher apoptotic rate with a 62% and 84% apoptotic rate at 0.1 and 0.5 μM, respectively (Figure 5b), compared to the apoptotic rate of 50 and 65% obtained with the combination of **15** and **16** ($P < 0.001$; Figure 5b).

Interestingly, comparative antiproliferative activities were recorded when testing **5** and **11** on an EGFR-wild-type H1299 adenocarcinoma NSCLC line, which overexpresses both SMO and MET receptors and is resistant to cisplatin treatment (see Supporting Information). Nevertheless, it should be mentioned that in this case the antiproliferative activity exerted by **5** and **11**, should not only be ascribed to the concurrent inhibition of SMO and MET. Indeed, in our previous inspection[7] we demonstrated that, in the same cell line, treatment with **15** and **16** (MET inhibitor and SMO antagonist, respectively) did not result in an efficient antiproliferative effect. In this respect, it should be outlined that while **5** and **11** demonstrated to be also potent AXL inhibitors, **15** is unable to inhibit this latter kinase. Therefore, it could be postulated that in the EGFR-wild-type H1299 adenocarcinoma NSCLC line the triple MET/SMO/AXL inhibition might be responsible for the enhanced antiproliferative activity of **5** and **11**. Indeed, the additional AXL inhibitory potency was also demonstrated to be responsible for the antiproliferative activity of **11** against HER2-positive breast tumor cells.[32] A further support for this hypothesis is provided by a recent paper by Qu et al demonstrating that AXL is indeed overexpressed in the H1299 adenocarcinoma NSCLC line and that silencing of this kinase inhibited cell proliferation and migration.[33] This might also explain

why in the HCC827-GR cell lines **5** and **11** are slightly more active than the concurrent treatment with **15** and **16** (Figure 5).

To study the influence of **5** and **11** on the activation/expression of key signaling mediators, we further characterized the effects of experimental compounds on the intracellular signaling by Western blotting. We used different doses according to the IC_{50} of each drug. As illustrated in Figure 6, treatment of HCC827-GR cells with **5** and **11**, for 72 hours, effectively blocked SMO and MET activation, confirming the dual inhibitory ability of these drugs. In addition, while not affecting the total MAPK and AKT protein levels, treatment with **5** and **11** markedly decrease the activated forms of both proteins, confirming our previous results[7] on the cooperation of Hh with MET pathway to the activation of both MAPK and AKT signaling pathways. In addition, vimentin expression, induced during the acquisition of gefitinib resistance, was significantly decreased after **5** or **11** treatment, suggesting that the Hh and MET pathways represent a key mediator of EMT in this model.
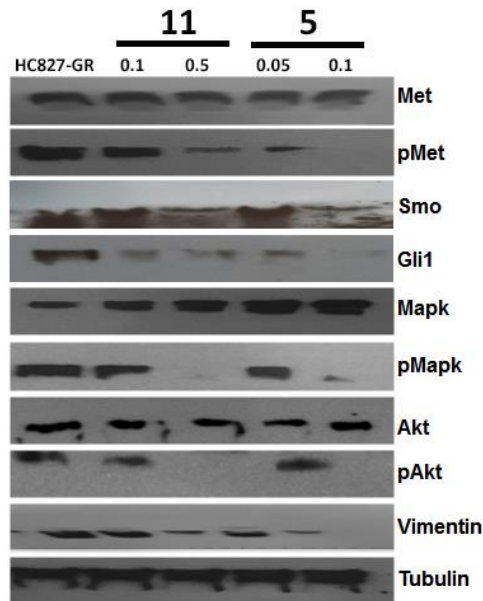
Figure 6. Effects on intracellular pathways by experimental compounds. Western blotting analysis of Hh and MET pathways following treatment with the indicated concentration of compound **5** and **11** on HCC827-GR NSCLC cell line. Tubulin was included as a loading control.

Dual MET/SMO modulators inhibit resistant human NSCLC tumor growth *in vivo*.

We previously demonstrated that the *in vivo* blockade of the Hh signaling pathway alone, or alternatively the sole MET pathway, is not sufficient to cause a significant delay in tumor growth whereas the concurrent inhibition of both pathways resulted in a substantial antitumor activity.[7] We, therefore, tested the efficacy of compounds **5** and **11**, as dual inhibitors of SMO and MET, to overcome the acquisition of resistance to the first-generation EGFR TKIs. Thus, HCC827 NSCLC tumor xenografts were implanted in nude mice and treated with gefitinib (*N*-(3-chloro-4-fluorophenyl)-7-methoxy-6-(3-morpholin-4-ylpropoxy)quinazolin-4-amine, **17**, Supplementary Chart S1).[34] Then, following tumor regrowth as resistance to **17** was acquired, mice were randomized to receive **5** or **11** +/- **17** (Figure 7). Indeed, treatment with **5** or **11** as single agents caused a significant decrease in tumor size. However, combined treatments of **17** plus **5** and **17** plus **11** significantly suppressed HCC827-**17** resistant tumor growth, suggesting that keeping the EGFR blockade during inhibition of SMO and MET is an effective strategy to overcome resistance to first-generation EGFR TKIs (Figure 7).

Subsequently, we also wanted to check if a similar strategy might be applied to EGFR-mutated NSCLC models with acquired resistance to third-generation EGFR inhibitors. We, therefore, performed a similar *in vivo* experiment inducing resistance to the third-generation inhibitor, osimertinib (*N*-(2-{[2-(dimethylamino)ethyl]-(methyl)amino}-4-methoxy-5-{[4-(1-methyl-1H-indol-3-yl)pyrimidin-2-yl]amino}phenyl)acrylamide, AZD9291, AstraZeneca, **18**, Supplementary Chart S1)[35] since analysis on resistant **18**-tumors harvested from treated mice, similarly to tumors

with acquired resistance to **17**, evidenced an activation of both Hh and MET pathways highlighting the role of those two pathways also in the resistance of third generation inhibitors.[8] Therefore, mice whose tumors are resistant to **18** treatment were randomized to treatment with **5** or **11** as single agents, or a combination of **5** or **11** with **18** (Figure 7). Interestingly, also HCC827-osimertinib resistant tumors resulted in being particularly sensitive to the dual inhibition of MET and SMO, and to a greater extent, to the triple inhibition of MET/SMO/EGFR (Figure 7).
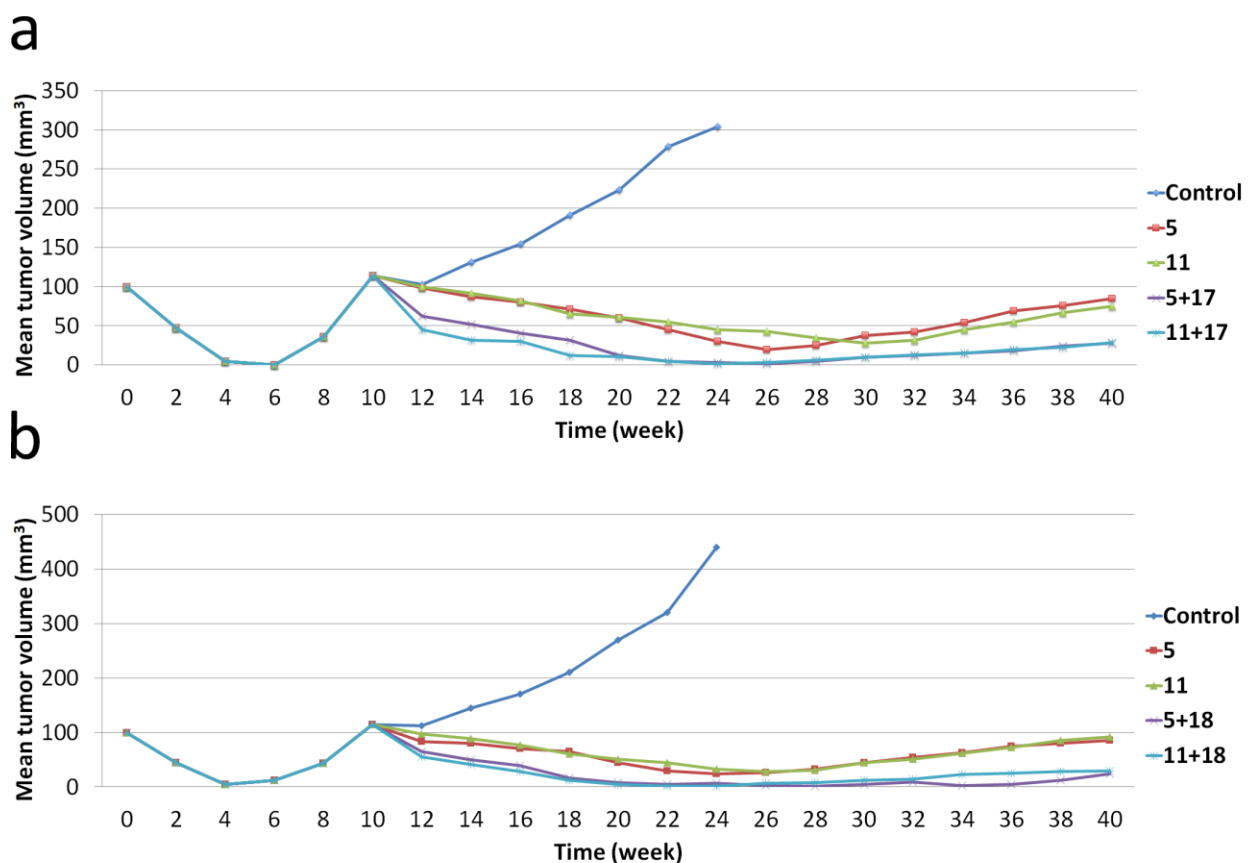

Figure 7. Effects of the treatment with compound **5** or **11** alone or in combination with **17** or **18** in human NSCLC tumor xenografts resistant to the EGFR-TKI. Mean tumor volumes of human NSCLC tumor xenografts made resistant to (**a**) **17** or (**b**) **18** and randomized to treatment with the

indicated drugs and combinations. Data represent the average (SD). Student t-test was used to compare tumor sizes among different treatment groups at day 21 following the start of treatment.

Conclusions

Our previous work[7] has highlighted the functional interaction of Hh and MET pathways and the importance of blocking both signaling pathways to revert EMT and enhance tumor sensitivity to anti-EGFR NSCLC models.

Stimulated by these findings, herein we were challenged to discover the first dual SMO/MET modulators that are able to overcome resistance to therapy in human NSCLC. Indeed, while these two pharmacological targets are unrelated from the structural point of view, they are able to recognize chemotypes that share common structural features. Thus, taking advantage of the published X-ray structures of the antagonist-bound SMO receptor a stepwise protocol of receptor-based VS was undertaken to *in silico* select, among a set of known MET inhibitors, the best candidates that can be recognized by the SMO receptor orthosteric binding site. Of the 12 tested compounds, 8 demonstrated the ability to displace **13** with nanomolar potency. These SMO binders were subsequently assayed in functional studies allowing the demonstration of their capacity to influence the SMO activation status in a concentration-dependent manner. Moreover, the efficacy of these compounds was reverted by the co-treatment with a known SMO agonist allowing us to further substantiate the antagonist activity of the 8 compounds. To the best of our knowledge, this is one of the first examples in which computational methods were successfully employed to rationally discover multi-target compounds hitting proteins belonging to phylogenetically and structurally distant families (namely the Frizzled class F) GPCRs and class IV tyrosine kinases receptors (TKR). Indeed, it should be mentioned that binding and functional assays were confined to the set of 25 compounds that were commercially available. Indeed, a large number of MET

inhibitors have been published and screened through our theoretical protocol that would deserve further experimental testing as SMO antagonists but were not considered in the present study because of their unavailability on the market. In this context, this study should also stimulate the biological evaluation of these latter compounds.

Prompted by these encouraging data, cell-based experiments were performed in NSCLC cell lines, made resistant to the EGFR-TKI **17**. Strikingly, in this model **5** and **11** were even more effective in achieving an antiproliferative effect than the combination treatment with a pure MET inhibitor and the SMO antagonist as well as the double silencing of the two target proteins. This result might be explained by the ability of **5** and **11** to inhibit AXL TKI. In this respect, both drugs were also the most active apoptosis inducers. When tested *in vivo*, **5** and **11** alone significantly decreased the tumor size of human NSCLC xenografts resistant to the EGFR-TKI, and this effect was potentiated by the co-administration with **17**. This demonstrates that, at least in our model, the triple inhibition of SMO, MET, and EGFR is indeed the most effective strategy to circumvent drug resistance to EGFR TKIs. The same data were also achieved by co-treatment with the selected drugs and third-generation EGFR TKIs, **18**.

Of note, our findings allow unraveling previous results achieved for **5** and **11**. In particular, it has been recently reported that **5**, when used in combination with erlotinib (EGFR-TKI) in a gastric cancer model, impairs the glycolysis pathway also by inhibiting the 6-phosphofructo-2-kinase/fructose-2,6-bisphosphatase 3 (PFKFB3) enzyme, thereby suggesting a novel mechanism of action for this drug.[36] In addition, it has been recently reported that the Hh signaling promotes glucose utilization and glycolysis, thereby accelerating cell proliferation in breast cancer cells, by positively modulating the 6-phosphofructo-2-kinase/fructose-2,6-bisphosphatase 3 (PFKFB3)

phosphorylation.[37] In this scenario, our data reconcile the negative modulation of cancer glycolysis exerted by **5** with its antagonist activity on SMO receptor.

On the other hand, **11** has been demonstrated to efficiently decrease tumor cell proliferation and to induce apoptosis in Hh-driven medulloblastomas. These data were first explained with the ability of this drug to inhibit MET that was proposed to be a marker of the aforementioned tumor.[38] Herein we suggest that the efficient antiproliferative activity displayed by **11** should also be ascribed to a direct interaction with the SMO receptor.

In conclusion, in this work the tandem application of predictive theoretical studies and in-depths *in vitro* and *in vivo* evaluation allowed us to identify from a large number of MET inhibitors those that can negatively modulate the SMO receptor and achieve superior antiproliferative effects in a model of resistant NSCLC tumor. In this context, the identification of **5** and **11** as negative modulators of the Hh pathway widens the range of action of these drugs in the context of NSCLC improving the already known AXL and MET targeting activity.

Experimental Section

Molecular Modelling. Proteins and ligands setup. The structure of the SMO receptor in complex with the antagonists (4-benzyl-piperazin-1-yl)-(3,5-dimethyl-1-phenyl-1*H*-pyrazol-4-ylmethylene)-amine[39] (SANT-1, PDB code 4N4W),[40] 2-(6-(4-(4-benzylphthalazin-1-yl)piperazin-1-yl)pyridin-3-yl)propan-2-ol[41] (ANTA XV, PDB code 4QIM),[40] 4-fluoro-*N*-methyl-*N*-(1-(4-(1-methyl-1*H*-pyrazol-5-yl)phthalazin-1-yl)piperidin-4-yl)-2-(trifluoromethyl)benzamide[42] (LY2940680, PDB code 4JKV)[43] and **13** (PDB code 4O9R)[44] were downloaded from the Protein Data Bank and prepared for docking calculations using the "Protein Preparation Wizard" panel of Schrödinger molecular modeling package.[45] In particular, using the "pre-process and analyze structure" tool, the bond orders and disulfide bonds were assigned, all the hydrogen atoms were

added, and water molecules were deleted. Using Epik 2.0, a prediction of the side chains hetero groups ionization and tautomeric states was performed.[46] An optimization of the hydrogen-bonding network was performed using the "H-bond assignment" tool. Finally, using the "impref utility", the positions of the hydrogen atoms were optimized by keeping all the heavy atoms in place.

A database of known MET ligands (1911 compounds) was subsequently prepared by interrogating the BindingDB database.[11] Ligands were prepared for docking using LigPrep.[47] Hydrogen atoms were added, ionizations states were generated, and tautomers were generated to prepare the required structures. All structures were then subjected to minimization using the OPLS-2005 force field. The same preparation was attained for the database of the known SMO antagonists downloaded from the BindingDB site.[11]

Docking calculations. According to the results of our very recent retrospective study, the employment of the AutoDock Vina docking software[48] when used against the ensemble of all the four receptors gave the best results in terms of enrichment factors (EF) when considering the lowest percentages of the ranked database (25%).[12] AutoDock Vina performances and accuracy are assured by a Lamarckian algorithm and an empirical binding free energy force field. Before the actual docking calculations could be run, both the database of ligands and the receptors had to be converted to the pdbqt format. The latter is very similar to a standard pdb but it includes 'Q' (partial charges) and 'T' atom types. Preparing the structures involves ensuring that its atoms are assigned the correct atom types, adding Gasteiger charges if necessary, merging non-polar hydrogens, detecting aromatic carbons, and setting up the 'torsion tree' in the case of ligands. Thus, the python scripts prepare_receptor4.py and prepare_ligand4.py, part of MGLTools[49,50] were employed applying the standard settings. After the preparation, the docking was performed using

the default settings of Vina, setting a box whose center and dimensions were identical to the one used in our previous work.[12] Results of these calculations produced four different rankings based on the predicted binding free energy (herein referred to as ΔG_{VINA}), one for each docking attained on the four receptor structures, which were subsequently unified using a parallel selection method. This selection method resulted in a ranking of the screened compounds in which ΔG_{VINA} values ranged from -6.5 to -14.8 kcal/mol.

Interaction fingerprints and interaction matrices of the SMO ligands against SMO receptors and MET ligands against the same receptors were calculated employing a routine of the Schröedinger 2015 release. The pose filter routine of the same release was used to count the number of interactions predicted for the MET compounds against D384, Y394, R400, E518, N219, F484, and W281 residues.

The fingerprint-based algorithm was used to cluster the 511 MET ligands in order to further refine them into 421 compounds. The canvas similarity and clustering, which is also part of the Schrodinger suite, was employed applying the following settings: the 8th atom typing scheme for the fingerprinting (atoms distinguished by ring size, aromaticity, HB acceptor/donor, ionization potential, whether terminal, whether halogen; bonds distinguished by bond order), Tanimoto as the similarity metric, and average as linkage as the clustering method. The same method (i.e. canvas similarity using the 8th atom typing scheme for the fingerprinting and Tanimoto as the similarity metric) was also used to evaluate the structural similarity between each of the 12 final compounds and any of the SMO antagonist reported in the BindingDB database.[11] Table S2 in Supporting Information reports the Tanimoto similarity index between the 12 compounds and the most similar SMO antagonist. These values range from 7.8% to 32% demonstrating that the selected ligands are structurally unrelated to the SMO antagonists described so far.

All of the pictures were rendered with the UCSF Chimera package from the Resource for Biocomputing, Visualization, and Informatics at the University of California, San Francisco.[37]

Prior to biological evaluation, the 12 compounds were screened for Pan Assay Interference Compounds using the PAINS-Remover web server (http://www.cbligand.org) that is a data analysis tools implemented for removal of PAINS compounds. All compounds passed this filtering with the exception of compound **7** and **9**. Compound **7** features an anil_di_alk_A substructure that is suggested to interfere with AlphaScreen® technology, possibly through efficient quenching of singlet oxygen.[52] In our case, we performed a radioligand displacement binding assay so no interference is expected. Compound **9** features an imine_one_isatin substructure which was found to interfere sometimes with the AlphaScreen® technology "for reasons unknown",[52] as stated by the authors. Also in this case, the tested ligand should not interfere with the implemented radioligand displacement binding assay. On the basis of NMR and MS analysis, all tested compounds have a purity ranging from 96 to 98%.

Cell lines and drugs. The human NSCLC HCC827 cell line was provided by American Type Culture Collection (ATCC, Manassas, VA, USA) and maintained in RPMI-1640 (Sigma-Aldrich, Saint Louis, MO, USA) medium supplemented with 10% fetal bovine serum (FBS; Life Technologies, Gaithersburg, MD) in a humidified atmosphere with 5% CO_2. The identity of all cell lines was confirmed by STR profiling (Promega, Madison, WV, USA) on an ad hoc basis prior to performing experiments. HCC827-GR (gefitinib Resistant) cell line was obtained *in vitro*, as previously described.[7] Briefly, over a period of 12 months, HCC827 cells were continuously exposed to increasing doses of **17**, starting from an IC_{50} dose that represented the dose to inhibit the growth of 50% of cells. HCC827-GR cells were maintained in culture with the maximum **17** dose that allowed cellular proliferation. The identity of cells was verified by STR profiling

(Promega) on an ad hoc basis prior to performing experiments, and repeated for all cell lines after a majority of the experiments were performed. Drugs gefitinib and sonidegib were purchased from Selleck Chemicals (Selleckchem, Houston, TX, USA). **18** was generously provided by Astra Zeneca.

SMO radioligand binding assays. Prior to binding experiments, all purchased compounds were analyzed to confirm the sample composition by LC/MS and ^{1}H NMR experiments. The binding experiments were performed as previously described with few modifications.[26] Briefly, HCC827-GR cells expressing V404M SMO receptors were grown in 24-well plates (100.000 cells/well) and fixed with 4% (v/v) formaldehyde/PBS for 20 min at room temperature (RT). Cells were subsequently incubated for 4 h at RT in binding buffer (Hanks balanced salt solution (HBSS) without Ca^{2+} and Mg^{2+} with glucose 1 g/L). Saturation binding experiments were performed using different [^{3}H]-**13** (American Radiolabeled Chemicals, Inc. Art. 1473 a.s. 20 Ci/mmol) concentrations ranging from 0.1 to 500 nM; in competition binding experiments cells were incubated with 25 nM [^{3}H]-**13** and different concentrations of the compounds. Non-specific binding was determined in the presence of 25 μM of compound **14**. Incubations were terminated by rapid washing with 1 mL binding buffer for three times. Then, the bound [^{3}H]-**13** was extracted in 200 μl of 0.1 N NaOH for 12 hours and neutralized with 200 μl of 0.1 N HCl. The amount of [^{3}H]-**13** in the extracts was measured using a scintillation counter. For the active compounds, the IC_{50} values were determined and Ki values were derived in accordance with the equation of Cheng and Prusoff.

The affinity of the compounds for the wild-type SMO was performed as previously described with few modifications.[26] Briefly, 15 μg of HEK293T-WT SMO membranes (Multispan Inc., Cod. MC1442; K_d = 20 nM; B_{max} = 6.2 pmol/mg protein) were incubated for 4 h at RT in binding buffer

(HEPES 50 mM, $MgCl_2$ 5 mM and BSA 0.02%) containing 25 nM $[^3H]$-**13** (American Radiolabeled Chemicals, Inc. Art. 1473 a.s. 20 Ci/mmol) and different concentrations of the compounds. Non-specific binding was determined in the presence of 25 μM of compound **14**. The bound radioactivity was separated by rapid filtration through GF/C glass fiber filters pre-soaked for 2 h in 0.3% polyethyleneimine pH 13.0 and washed three times with 4 mL of ice-cold phosphate-buffered saline with 0.01% Triton X-100, pH 7.0. Radioactivity was measured by liquid scintillation spectrometry. Dose-response curves are reported in Supporting Information Figures S8 and S9.

Luciferase Assay. Here, we performed GLI1 luciferase assay to test the influence of selected compounds on GLI1 activity in HCC827-GR cells by using the Dual-Luciferase Assay system (Promega), following the manufacturer's protocol. For each experiment, a total of $5x10^5$ cells were seeded in FBS-free medium in 24-well plates and transfection started when cells reach a confluency of 50%. We co-transfected the cells with the GLI1-Luc reporter plasmid (400 ng/well), kindly provided by Dr. Mariolina Castellone[53] (University of Naples Federico II) and pRL-TK, Renilla reporter, encoding the Renilla luciferase (Promega), to normalize the results. In GLI1 reporter vector, the transcription of Firefly luciferase gene is under the control of a promoter region specific for the transcription factor GLI1, so GLI1 luciferase activity correlates with the binding of GLI1 to its promoter region; in control reporter, Renilla luciferase activity depends on a constitutive promoter (thymidine kinase). The transfection was done in triplicate using Lipofectamine 2000 (provided by Thermo Fisher Scientific) as transfection reagent, according to manufacturer' instructions. The medium of transfection was replaced after 8 h with culture medium, containing the indicated MET ligands or without the SMO agonist SAG (100 nM) [*N*-

methyl-N'-(3-pyridinylbenzyl)-N'-(3-chlorobenzo[b]thiophene-2-carbonyl)-1,4-diaminocyclohexane], purchased from Sigma-Aldrich.

Firefly luciferase is a protein from Photinus Pyralis that reacts with its substrate (beetle luciferin, ATP, magnesium, and molecular oxygen) creating luminescence, measured by the luminometer Autolumat LB 953 (EG&G, Berthold, Bad Wildbad, Germany). According to the protocol of the kit Dual-Luciferase® Reporter Assay System (Promega), after about 48 hours from transfection, we removed the medium and washed once with PBS. Then, we added 100 µl of Lysis Buffer 1X in each well shaking for 20 minutes at RT and finally scraped.

For the measurement of GLI1 luciferase activity, we mixed by pipetting 30 µl of lysated cells and 30 µl of Luciferase Assay Reagent, containing its substrate for reaction. After the reading at luminometer and the record of data, we added 30 µl of Stop and Glo Reagent, which blocked GLI1 induced firefly luciferase signal and contained Renilla luciferase substrate, and repeated the luminometer measurement to obtain the control values. For the analysis of data, we calculated the average values of GLI1 luciferase signal, normalized to Renilla luciferase values, and represented the results as fold change with respect to control cells and cells transfected with the empty vector; results were the average of three independent experiments.

Protein expression analysis. Protein lysates were obtained by homogenization in RIPA lysis buffer (0.1% sodium dodecyl sulfate (SDS), 0,5% deoxycholate, 1%Nonidet, 100mmol/L NaCl, 10 mmol/L Tris–HCl (pH 7.4), 0.5 mmol/L dithiothreitol, and 0.5% phenylmethylsulfonyl fluoride, protease inhibitor cocktail (Hoffmann-La Roche) and clarification by centrifugation at 14,000 rpm for 10 minutes a 4°C. Cancer cells were lysed with Tween-20 lysis buffer (50 mmol/L HEPES, pH 7.4, 150 mmol/L NaCl, 0.1% Tween-20, 10% glycerol, 2.5 mmol/L EGTA, 1 mmol/L EDTA, 1 mmol/L DTT, 1 mmol/L phenylmethylsulfonyl fluoride, and 10 µg/mL of leupeptin and

aprotinin). Protein lysates containing comparable amounts of proteins, estimated by a modified Bradford assay (Bio-Rad), were subjected to Western blot analysis, as previously described.[7] Immunocomplexes were detected with the enhanced chemiluminescence kit ECL plus, by Thermo Fisher Scientific (Rockford, IL). Desired proteins were probed with corresponding antibodies. Primary antibodies for western blot analysis against p-MAPK44/42 (Thr202/Tyr204), MAPK44/42, p-AKT (Ser473), AKT, p-MET (Tyr1234/1235), MET, SMO, GLI1 were obtained from Cell Signaling Technology; monoclonal anti-α-tubulin antibody (T8203) from Sigma Chemical Co. The following secondary antibodies from Bio-Rad were used: goat anti-rabbit IgG and rabbit anti-mouse IgG. Immunoreactive proteins were visualized by enhanced chemiluminescence (ECL plus; Thermo Fisher Scientific). Each experiment was done in triplicate.

Cell proliferation assays. Cancer cells were seeded in 96-multiwell plates and were treated with different doses of indicated drugs for 72 hours. Cell proliferation was measured with the MTT assay, as previously described.[7] IC_{50} values were determined by interpolation from the dose-response curves. Results represent the median of three separate experiments, each performed in quadruplicate. Synergism was calculated with ComboSyn software, ComboSyn Inc., Paramus, NK. 07652 USA.

RNA Silencing. The small inhibitor duplex RNAs (siRNA) (ON-target plus SMARTpool) siSMO, siMET and siCONTROL Non-targeting Pool (#D-001206-13-05), used as a negative (scrambled) control, were provided from Dharmacon (Lafayette, CO). Cells were transfected with 100 nM siRNAs using Dharmafect reagent following manufacturer's instructions. The day before transfection, the cells were plated in 35 mm dishes at 40% of confluence in medium supplemented with 5% FBS without antibiotics. Where necessary, cells were treated with different compounds,

as previously described; 24 hours before harvesting and cell proliferation or western blot analysis were then performed.

Assessment of apoptosis. Apoptosis was detected by flow cytometry via the examination of altered plasma membrane phospholipid packing by lipophilic dye Annexin V as described elsewhere.[7] Briefly, treated cells were harvested by trypsin, washed twice with PBS, and were then resuspended in binding buffer at a concentration of 1×10^6 cells/mL according to the manufacturer's instruction. Thereafter, 5 µL of Annexin V-FITC and 5 µL of propidium iodide were added into 100 µL of cell suspension and incubated for 30 min at room temperature in the dark. After adding 400 µL of binding buffer, labeled cells were counted by flow cytometry within 30 min. All early apoptotic cells (Annexin V–positive, propidium iodide–negative), necrotic/late apoptotic cells (double positive), as well as living cells (double negative), were detected by FACSCalibur flow cytometer and subsequently analyzed by Cell Quest software (Becton Dickinson). Argon laser excitation wavelength was 488 nm, whereas emission data were acquired at wavelength 530 nm (FL-1 channel) for FITC and 670 nm (FL-3 c3 channel) for propidium iodide.

In vivo experiments. 4- to 6-week old female balb/c athymic (nuþ/nuþ) mice were purchased from Charles River Laboratories. The research protocol was approved and mice were maintained in accordance with the Institutional Guidelines of the University of Campania Luigi Vanvitelli Animal Care and Use Committee. Mice were acclimatized for 1 week before being injected with cancer cells and injected subcutaneously with 10^7 HCC827 cells that had been diluted in **200** µL of Matrigel (Corning Life Sciences, MA, USA), 1:1 in the culture medium. For induction of resistance to **17** or **18**, when tumors reached a mean volume of 150 mm³, mice were treated with escalating doses of **17** (from 18.7 mg/kg/day to 150 mg/kg/day: 3 weeks with 18.7 mg/kg/day, 3

weeks with 37,5 mg/kg/day, 3 weeks with 75 mg/kg/day and last 3 weeks with 150 mg/kg/day) or **198** (with the same protocol of escalating doses every three weeks: 5 mg/kg/day for the first three weeks, 10 mg/kg/day for following three weeks, 17,5 mg/kg/day for subsequent three weeks and 25 mg/kg daily for last three weeks orally) over 4 months to derive **17/18**-resistant tumors (defined as >25% re-growth from max reduction). At the end of treatment period, resistant tumors were randomized into one of the following four arms: control, **5**, **11**, **17/18** plus **5**, **17/18** plus **11**. **17** and **18** were continued at maximum dose reached before resistance, **5** and **11** were used as single agents and in combination at fixed doses of 15 mg/kg/day and 20 mg/kg/day orally, respectively. Body weight and tumor volume were monitored on alternate days. Tumor volume was measured using the formula $\pi/6$ larger diameter x (smaller diameter)^2. Characterization of the pharmacokinetics of **11** have been already reported by Faria et al. demonstrating that this compound reaches the maximum plasma concentration after 5 hours from oral administration.[38] Characterization of the pharmacokinetics of **5** demonstrated that this drug reaches a plasma concentration of 0.8 μM when orally administered in mice (20 mg/kg).

ASSOCIATED CONTENT

Supporting Information.

The Supporting Information is available free of charge on the ACS Publications website at DOI: XXXXXXX.

Additional Tables S1 and S2, Figures S1-S10, and compound characterization (PDF).

Molecular formula strings and some data (CSV).

Coordinates of the calculated SMO/ligand complexes (PDB).

AUTHOR INFORMATION

Corresponding Authors

*S.C. Phone: +39 0823 274789. E-mail: sandro.cosconati@unicampania.it. F.M. Phone: +39 081 5666732. E-mail: florianamorgillo@yahoo.com.

Author Contributions

The manuscript was written through contributions of all authors. All authors have given approval to the final version of the manuscript. [†]These authors contributed equally to this work.

ABBREVIATIONS

TKI, Tyrosine kinase inhibitors; EGFR, EGF receptor; NSCLC, non-small cell lung cancer; EMT, epithelial-to-mesenchymal transition; Hh, Hedgehog; SMO, Smoothened; TCGA, the cancer genome atlas; HGFR, hepatocyte growth factor receptor; GR, gefitinib resistant;

REFERENCES

1. Jemal, A.; Siegel, R.; Ward, E.; Hao, Y.; Xu, J.; Thun, M. J. Cancer Statistics, 2009. *CA Cancer J. Clin.* **2009**, *59*, 225–249.

2. Yang, L.; Xie, G.; Fan, Q.; Xie, J. Activation of the hedgehog-signaling pathway in human cancer and the clinical implications. *Oncogene* **2010**, *29*, 469–481.

3. Z. Yuan, Z.; Goetz, J. A.; Singh, S.; Ogden, S. K.; Petty, W. J.; Black, C. C.; Memoli, V. A.; Dmitrovsky, E.; Robbins, D. J. Frequent requirement of hedgehog signaling in non-small cell lung carcinoma. *Oncogene* **2006**, *26*, 1046–1055.

4. Ahmad, A.; Maitah, M. I. Y.; Ginnebaugh, K. R.; Li, Y.; Bao, B.; Gadgeel, S. M.; Sarkar, F. H. Inhibition of hedgehog signaling sensitizes NSCLC cells to standard therapies through modulation of EMT-regulating miRNAs. *J. Hematol. Oncol.* **2013**, *6* , 77.

5. Tsao, A.; Byers, L. A.; Diao, L.; Wang, J.; Weinstein, J. N.; Meric-Bernstam, F.; Aldape, K.; Heymach, J. V. P2.06-032-SMO mutations occur in non-small cell lung cancer (NSCLC) and may respond to hedgehog inhibitors. *15th World Conference on Lung Cancer* 2013, in Sydney Australia.

6. Reungwetwattana, T.; Liang, Y.; Zhu, V.; Ou, S. I. The race to target MET exon 14 skipping alterations in non-small cell lung cancer: the why, the how, the who, the unknown, and the inevitable. *Lung Cancer.* **2017**, *103*, 27–37.

7. Della Corte, C. M.; Bellevicine, C.; Vicidomini, G.; Vitagliano, D.; Malapelle, U.; Accardo, M.; Fabozzi, A.; Fiorelli, A.; Fasano, M.; Papaccio, F.; Martinelli, E.; Troiani, T.; Troncone, G.; Santini, M.; Bianco, R.; Ciardiello, F.; Morgillo, F. SMO gene amplification and activation of the hedgehog pathway as novel mechanisms of resistance to anti-epidermal growth factor receptor drugs in human lung cancer. *Clin. Cancer Res.* **2015**, *21*, 4686–4697.

8. Della Corte, C. M.; Malapelle, U.; Vigliar, E.; Pepe, F.; Troncone, G.; Ciaramella, V.; Troiani, T.; Martinelli, E.; Belli, V.; Ciardiello, F.; Morgillo, F. Efficacy of continuous EGFR-inhibition and role of hedgehog in EGFR acquired resistance in human lung cancer cells with activating mutation of EGFR. *Oncotarget* **2017**, *8*, 23020–23032.

9. Anighoro, A.; Bajorath, J.; Rastelli, G. Polypharmacology: challenges and opportunities in drug discovery. *J. Med. Chem.* **2014**, *57,* 7874–7887.

10. Nosengo, N. Can you teach old drugs new tricks? *Nature* **2016**, *534*, 314–316.

11. Liu, T.; Lin, Y.; Wen, X.; Jorissen, R. N.; Gilson, M. K. BindingDB: a web-accessible database of experimentally determined protein-ligand binding affinities. *Nucleic Acids Res.* **2007**, *35*, 198–201.

12. Amendola, G.; Di Maio, D.; La Pietra, V.; Cosconati, S. Best matching protein conformations and docking programs for a virtual screening campaign against SMO receptor. *Mol. Inf.* **2016**, *35*, 340–349.

13. Wang, C.; Wu, H.; Evron, T.; Vardy, E.; Han, G. W.; Huang, X.P.; Hufeisen, S. J.; Mangano, T. J.; Urban, D. J.; Katritch, V.; Cherezov, V.; Caron, M. G.; Roth, B. L.; Stevens, R. C. Structural basis for smoothened receptor modulation and chemoresistance to anticancer drugs. *Nat. Commun.* **2014**, *5*, 4355.

14. Ishikawa, T.; Seto, M.; Banno, H.; Kawakita, Y.; Oorui, M.; Taniguchi, T.; Ohta, Y.; Tamura, T.; Nakayama, A.; Miki, H.; Kamiguchi, H.; Tanaka, T.; Habuka, N.; Sogabe, S.; Yano, J.; Aertgeerts, K.; Kamiyama, K. Design and synthesis of novel human epidermal growth factor receptor 2 (HER2)/epidermal growth factor receptor (EGFR) dual inhibitors bearing a pyrrolo[3,2-d]pyrimidine scaffold. *J. Med. Chem.* **2011**, *54*, 8030–8050.

15. Liang, Z.; Zhang, D.; Ai, J.; Chen, L.; Wang, H.; Kong, X.; Zheng, M.; Liu, H.; Luo, C.; Geng, M.; Jiang, H.; Chen, K. Identification and synthesis of N′-(2-oxoindolin-3-ylidene)hydrazide derivatives against c-Met kinase. *Bioorg. Med. Chem Lett.* **2011**, *21*, 3749–3754.

16. Schmidt, S.; Preu, L.; Lemcke, T.; Totzke, F.; Schächtele, C.; Kubbutat, M. H.; Kunick, C. Dual IGF-1R/SRC inhibitors based on a N′-aroyl-2-(1H-indol-3-yl)-2-oxoacetohydrazide structure. *Eur. J. Med. Chem.* **2011**, *46*, 2759–2769.

17. Claridge, S.; Raeppel, F.; Granger, M.-C.; Bernstein, N.; Saavedra, O.; Zhan, L.; Llewellyn, D.; Wahhab, A.; Deziel, R.; Rahil, J.; Beaulieu, N.; Nguyen, H.; Dupont, I.; Barsalou, A.; Beaulieu, C.; Chute, I.; Gravel, S.; Robert, M.-F.; Lefebvre, S.; Dubay, M.; Pascal, R.; Gillespie, J.; Jin, Z.; Wang, J.; Besterman, J. M.; Macleod, A. R.; Vaisburg, A. Discovery of a novel and potent series of thieno[3,2-b]pyridine-based inhibitors of c-Met and VEGFR2 tyrosine kinases. *Bioorg. Med. Chem Lett.* **2008**, *18*, 2793–2798.

18. Schroeder, G. M.; An, Y.; Cai, Z.-W.; Chen, X.-T.; Clark, C.; Cornelius, L. A. M.; Dai, J.; Gullo-Brown, J.; Gupta, A.; Henley, B.; Hunt, J. T.; Jeyaseelan, R.; Kamath, A.; Kim, K.; Lippy, J.; Lombardo, L. J.; Manne, V.; Oppenheimer, S.; Sack, J. S.; Schmidt, R. J.; Shen,

G.; Stefanski, K.; Tokarski, J. S.; Trainor, G. L.; Wautlet, B. S.; Wei, D.; Williams, D. K.; Zhang, Y.; Zhang, Y.; Fargnoli, J.; Borzilleri, R. M. Discovery of N-(4-(2-amino-3-chloropyridin-4-yloxy)-3-fluorophenyl)-4-ethoxy-1-(4-fluorophenyl)-2-oxo-1,2-dihydropyridine-3-carboxamide (BMS-777607), a selective and orally efficacious inhibitor of the Met kinase superfamily. *J. Med. Chem.* **2009**, *52*, 1251–1254.

19. Guagnano, V.; Furet, P.; Spanka, C.; Bordas, V.; Douget, M. L.; Stamm, C.; Brueggen, J.; Jensen, M. R.; Schnell, C.; Schmid, H.; Wartmann, M.; Berghausen, J.; Drueckes, P.; Zimmerlin, A.; Bussiere, D.; Murray, J.; Porta, D. G. discovery of 3-(2,6-dichloro-3,5-dimethoxy-phenyl)-1-{6-[4-(4-ethyl-piperazin-1-yl)-phenylamino]-pyrimidin-4-yl}-1-methyl-urea (NVP-BGJ398), a potent and selective inhibitor of the fibroblast growth factor receptor family of receptor tyrosine kinase. *J. Med. Chem.* **2011**, *54*, 7066–7083.

20. Rowbottom, M. W.; Faraoni, R.; Chao, Q.; Campbell, B. T.; Lai, A. G.; Setti, E.; Ezawa, M.; Sprankle, K. G.; Abraham, S.; Tran, L.; Struss, B.; Gibney, M.; Armstrong, R. C.; Gunawardane, R. N.; Nepomuceno, R. R.; Valenta, I.; Hua, H.; Gardner, M. F.; Cramer, M. D.; Gitnick, D.; Insko, D. E.; Apuy, J. L.; Jones-Bolin, S.; Ghose, A. K.; Herbertz, T.; Ator, M. A.; Dorsey, B. D.; Ruggeri, B.; Williams, M.; Bhagwat, S.; James, J.; Holladay, M. W. Identification of 1-(3-(6,7-dimethoxyquinazolin-4-yloxy)phenyl)-3-(5-(1,1,1-trifluoro-2-methylpropan-2-yl)isoxazol-3-yl)urea hydrochloride (CEP-32496), a highly potent and orally efficacious inhibitor of V-RAF murine sarcoma viral oncogene homologue b1 (BRAF) V600E. *J. Med. Chem.* **2012**, *55*, 1082–1105.

21. Davis, M. I.; Hunt, J. P.; Herrgard, S.; Ciceri, P.; Wodicka, L. M.; Pallares, G.; Hocker, M.; Treiber, D. K.; Zarrinkar, P. P. Comprehensive analysis of kinase inhibitor selectivity. *Nat. Biotech.* **2011**, *29*, 1046–1051.

22. Qian, F.; Engst, S.; Yamaguchi, K.; Yu, P.; Won, K.-A.; Mock, L.; Lou, T.; Tan, J.; Li, C.; Tam, D.; Lougheed, J.; Yakes, F. M.; Bentzien, F.; Xu, W.; Zaks, T.; Wooster, R.; Greshock, J.; Joly, A. H. Inhibition of tumor cell growth, invasion, and metastasis by EXEL-2880 (XL880, GSK1363089), a novel inhibitor of HGF and VEGF receptor tyrosine kinases. *Cancer Res.* **2009**, *69*, 8009–8016.

23. Albert, D.H.; Tapang, P.; Magoc, T. J.; Pease, L. J.; Reuter, D. R.; Wei, R. Q.; Li, J.; Guo, J.; Bousquet, P. F.; Ghoreishi-Haack, N. S.; Wang, B.; Bukofzer, G. T.; Wang, Y. C.; Stavropoulos, J. A.; Hartandi, K.; Niquette, A. L.; Soni, N.; Johnson, E. F.; McCall, J. O.;

Bouska, J. J.; Luo, Y.; Donawho, C. K.; Dai, Y.; Marcotte, P. A.; Glaser, K. B.; Michaelides, M. R.; Davidsen, S. K. Preclinical activity of ABT-869, a multitargeted receptor tyrosine kinase inhibitor. *Mol. Cancer. Ther.* **2006,** *5*, 995-1006.

24. Chen, J. K.; Taipale, J.; Cooper, M. K.; Beachy, P. A. Inhibition of hedgehog signaling by direct binding of cyclopamine to Smoothened. *Genes Dev.* **2002**, 16, 2743–2274.

25. Gunzner, J.; Sutherlin, D.; Stanley, M.; Bao, L.; Castanedo, G.; Lalonde, R.; Wang, S.; Reynolds, M.; Savage, S.; Malesky, K.; Dina, M. Preparation of arylpyridines as inhibitors of hedgehog signalling. PCT Int. Appl. WO 2006028958 A2, March 16, **2006**.

26. Wang, J.; Mook, R. A.; Lu, J.; Gooden, D. M.; Ribeiro, A.; Guo, A.; Barak, L. S.; Lyerly, H. K.; Chen, W. Identification of a novel smoothened antagonist that potently suppresses hedgehog signaling. *Bioorg. Med. Chem.* **2012**, *20*, 6751–6757.

27. Rahnama, F.; Shimokawa, T.; Lauth, M.; Finta, C.; Kogerman, P.; Teglund, S.; Toftgård, R.; Zaphiropoulos, P. G. Inhibition of GLI1 gene activation by Patched1. *Biochem. J.* **2006**, *394*, 19–26.

28. Frank-Kamenetsky, M.; Zhang, X. M.; Bottega, S.; Guicherit, O.; Wichterle, H.; Dudek, H.; Bumcrot, D.; Wang, F.Y.; Jones, S.; Shulok, J.; Rubin, L. L.; Porter, J. A. Small-molecule modulators of Hedgehog signaling: identification and characterization of Smoothened agonists and antagonists. *J. Biol.* **2002**, *1*, 10.

29. Rosell, R.; Wannesson, L. A genetic snapshot of small cell lung cancer. *Cancer Discov.* **2012**, *2*, 769–771.

30. Pan, S.; Wu, X.; Jiang, J.; Gao, W.; Wan, Y.; Cheng, D.; Han, D.; Liu, J.; Englund, N. P.; Wang, Y.;Peukert, S.; Miller-Moslin, K.; Yuan, J.; Guo, R.; Matsumoto, M.; Vattay, A.; Jiang, Y.; Tsao, J.; Sun, F.; Pferdekamper, A. C.; Dodd, S.; Tuntland, T.; Maniara, W.; Kelleher, J. F., 3rd; Yao, Y. M.; Warmuth, M.;Williams, J.; Dorsch, M. Discovery of NVP-LDE225, a potent and selective smoothened antagonist. *ACS Med. Chem. Lett.* **2010**, 1, 130–134.

31. Christensen, J. G.; Schreck, R.; Burrows, J.; Kuruganti, P.; Chan, E.; Le, P.; Chen, J.; Wang, X.; Ruslim, L.; Blake, R.; Lipson, K. E.; Ramphal, J.; Do, S.; Cui, J. J.; Cherrington, J. M.; Mendel, D. B. A selective small molecule inhibitor of MET kinase inhibits METdependent phenotypes in vitro and exhibits cytoreductive antimutor activity in vivo. *Cancer Res.* **2003**, *63*, 7345–7355.

32. Liu, L.; Greger, J.; Shi, H.; Liu, Y.; Greshock, J.; Annan, R.; Halsey, W.; Sathe, G. M.; Martin, A.-M.; Gilmer, T. M. Novel mechanism of lapatinib resistance in HER2-positive breast tumor cells: activation of AXL. *Cancer Res.* **2009**, *69*, 6871–6878.

33. Qu, X.; Liu, J.; Zhong, X.; Li, X.; Zhang, Q. Role of AXL expression in non-Small cell lung cancer. *Oncol. Lett.* **2016**, *12*, 5085–5091.

34. Xu, T.; Peng, T.; Ren, X.; Zhang, L.; Yu, L.; Luo, J.; Zhang, Z.; Tu, Z.; Tong, L.; Huang, Z.; Lu, X.; Geng, M.;Xie, H.; Ding, J.; Ding, K. C5-substituted pyrido[2,3-*d*]pyrimidin-7-ones as highly specific kinase inhibitors targeting the clinical resistance-related EGFR^{T790M} mutant. *MedChemComm* **2015**, 6, 1693–1697.

35. Cross, D. A. E.; Ashton, S. E.; Ghiorghiu, S.; Eberlein, C.; Nebhan, C. A.; Spitzler, P. J.; Orme, J. P.; Finlay, M. R. V.; Ward, R. A.; Mellor, M. J.; Hughes, G.; Rahi, A.; Jacobs, V. N.; Brewer, M. R.; Ichihara, E.; Sun, J.; Jin, H.; Ballard, P.; Al-Kadhimi, K.; Rowlinson, R.; Klinowska, T.; Richmond, G. H. P.; Cantarini, M.; Kim, D. W.; Ranson, M. R.; Pao, W. AZD9291, an irreversible EGFR TKI, overcomes T790M-mediated resistance to EGFR inhibitors in lung cancer. *Cancer Discovery* **2014**, *4*, 1046–1061.

36. Bonfils, C.; Beaulieu, N.; Fournel, M.; Ste-Croix, H.; Besterman, J. M.; Maroun, C. R. The combination of MGCD265, a Met/VEGFR inhibitor in clinical development, and erlotinib potently inhibits tumor growth by altering multiple pathways including glycolysis. *Cancer Res.* **2012**, *72*, 1790–1790.

37. Ge, X.; Lyu, P.; Gu, Y.; Li, L.; Li, J.; Wang, Y.; Zhang, L.; Fu, C.; Cao, Z. Sonic hedgehog stimulates glycolysis and proliferation of breast cancer cells: modulation of PFKFB3 activation. *Biochem. Biophys. Res. Comm.* **2015**, *464*, 862–868.

38. Faria, C. C.; Golbourn, B. J.; Dubuc, A. M.; Remke, M.; Diaz, R. J.; Agnihotri, S.; Luck, A.; Sabha, N.; Olsen, S.; Wu, X.; Garzia, L.; Ramaswamy, V.; Mack, S. C.; Wang, X.; Leadley, M.; Reynaud, D.; Ermini, L.; Post, M.; Northcott, P. A.; Pfister, S. M.; Croul, S. E.; Kool, M.; Korshunov, A.; Smith, C. A.; Taylor, M. D.; Rutka, J. T. Foretinib is effective therapy for metastatic sonic hedgehog medulloblastoma. *Cancer Res.* **2014**, *75*, 134–146.

39. Chen, J. K.; Taipale, J.; Young, K. E.; Maiti, T.; Beachy, P. A. Small molecule modulation of smoothened activity. *Proc. Natl. Acad. Sci. USA* **2002**, *99*, 14071–14076.

40. Wang, C.; Wu, H.; Evron, T.; Vardy, E.; Han, G. W.; Huang, X.-P.; Hufeisen, S. J.; Mangano, T. J.; Urban, D. J.; Katritch, V.; Cherezov, V.; Caron, M. G.; Roth, B. L.;

Stevens, R. C. Structural basis for smoothened receptor modulation and chemoresistance to anticancer drugs. *Nat. Commun.* **2014**, *5*, 4355.

41. Miller-Moslin, K.; Peukert, S.; Jain, R. K.; McEwan, M. A.; Karki, R.; Llamas, L.; Yusuff, N.; He, F.; Li, Y.;Sun, Y.; Dai, M.; Perez, L.; Michael, W.; Sheng, T.; Lei, H.; Zhang, R.; Williams, J.; Bourret, A.; Ramamurthy, A.; Yuan, J.; Guo, R.; Matsumoto, M.; Vattay, A.; Maniara, W.; Amaral, A.; Dorsch, M.; Kelleher, J. F., III.1-Amino-4-benzylphthalazines as orally bioavailable smoothened antagonists with antitumor activity. *J. Med. Chem.* **2009**, *52*, 3954–3968.

42. Hipskind, P. A.; Patel, B. K.; Wilson, T. Preparation of disubstituted phthalazine derivatives for use as hedgehog pathway antagonists and useful in treatment of cancer. PCT Int. Appl. WO 2010147917 A1, Dec 23, **2010.**

43. Wang, C.; Wu, H.; Katritch, V.; Han, G. W.; Huang, X.-P.; Liu, W.; Siu, F. Y.; Roth, B. L.; Cherezov, V.; Stevens, R. C. Structure of the human smoothened receptor bound to an antitumour agent. *Nature* **2013**, *497*, 338–343.

44. Weierstall, U.; James, D.; Wang, C.; White, T. A.; Wang, D.; Liu, W.; Spence, J. C. H.; Doak, R. B.; Nelson, G.; Fromme, P.; Fromme, R.; Grotjohann, I.; Kupitz, C.; Zatsepin, N. A.; Liu, H.; Basu, S.; Wacker, D.; Han, G. W.; Katritch, V.; Boutet, S.; Messerschmidt, M.; Williams, G. J.; Koglin, J. E.; Seibert, M. M.; Klinker, M.; Gati, C.; Shoeman, R. L.; Barty, A.; Chapman, H. N.; Kirian, R. A.; Beyerlein, K. R.; Stevens, R. C.; Li, D.; Shah, S. T. A.; Howe, N.; Caffrey, M.; Cherezov, V. Lipidic cubic phase injector facilitates membrane protein serial femtosecond crystallography. *Nat. Commun.* **2014**, *5*, 3309.

45. Maestro, version 10; Schrödinger, LLC: New York, 2015; http://www.schrodinger.com/.

46. Epik, version 2.2; Schrodinger, LLC: New York, 2011.

47. LigPrep, version 2.5; Schrödinger, LLC: New York, 2011.

48. Trott, O.; Olson, A. J. AutoDock Vina: improving the speed and accuracy of docking with a new scoring function, efficient optimization, and multithreading. *J. Comput. Chem.* **2009**, 455–461.

49. Morris, G. M.; Huey, R.; Lindstrom, W.; Sanner, M. F.; Belew, R. K.; Goodsell, D. S.; Olson, A. J. AutoDock4 and AutoDockTools4: automated docking with selective receptor flexibility. *J. Comput. Chem.* **2009**, *30*, 2785–2791.

50. Sanner, M. F. Python: a programming language for software integration and development, *J. Mol. Graph. Mod.* **1999**, *17*, 57–61.

51. Pettersen, E. F.; Goddard, T. D.; Huang, C. C.; Couch, G. S.; Greenblatt, D. M.; Meng, E. C.; Ferrin, T. E. UCSF Chimera: a visualization system for exploratory research and analysis. *J. Comput. Chem.* **2004**, *25*, 1605–1612.

52. Baell, J. B.; Holloway, G. A. New substructure filters for removal of pan assay interference compounds (pains) from screening libraries and for their exclusion in bioassays. *J. Med. Chem.* **2010**, *53*, 2719–2740.

53. Castellone, M. D.; Laukkanen, M. O.; Teramoto, H.; Bellelli, R.; Alì, G.; Fontanini, G.; Santoro, M.; Gutkind, J. S. Cross talk between the bombesin neuropeptide receptor and sonic hedgehog pathways in small cell lung carcinoma. *Oncogene* **2014**, *34*, 1679–1687.

54. Fournel, M.; Dupont, I.; Bonfils, C.; Dubay, M.; Ste-Croix, H.; Beaulieu, C.; Beaulieu, N.; Lemoyne, C.; Wang, J.; Isakovic, L.; Claridge, S.; Saavedra, O.; Raeppel, F.; Raeppel, S.; Mannion, M.; Vaisburg, A.; Martell, R. E.; Besterman, J. M.; Maroun, C. Potent preclinical antitumor activity of MGCD265, an orally active Met/VEGFR multitargeted kinase inhibitor in phase II clinical development, in combination with an EGFR Inhibitor. *Cancer Res.* **2014**, *70*, 3612–3612.

Table of Contents graphic